α-dystroglycan and is upregulated in dystrophic muscle. *J. Cell Biol.* 148, 801–810
28 Henry, M.D. and Campbell, K.P. (1998) A role for dystroglycan in basement membrane assembly. *Cell* 95, 859–870
29 Durbeej, M. and Ekblom, P. (1997) Dystroglycan and laminins: glycoconjugates involved in branching epithelial morphogenesis. *Exp. Lung Res.* 23, 109–118
30 Brown, S.C. *et al.* (1999) Dystrophic phenotype induced *in vitro* by blockade of muscle α-dystroglycan-laminin interaction. *J. Cell Sci.* 112, 209–216
31 Leschziner, A. *et al.* (2000) Neural regulation of α-dystroglycan biosynthesis and glycosylation in skeletal muscle. *J. Neurochem.* 74, 70–80
32 Colognato, H. *et al.* (1999) Laminin polymerisation induces a receptor-cytoskeleton network. *J. Cell Biol.* 145, 619–631
33 Fallon, J.R. and Hall, Z.W. (1994) Building synapses: agrin and dystroglycan stick together. *Trends Neurosci.* 17, 469–473
34 Sealock, R. and Froehner, S.C. (1994) Dystrophin-associated proteins and synapse formation: Is α-dystroglycan the agrin receptor? *Cell* 77, 617–619
35 Henry, M.D. and Campbell, K.P. (1996) Dystroglycan – an extracellular-matrix receptor-linked to the cytoskeleton. *Curr. Opin. Cell Biol.* 8, 625–631
36 Gautam, M. *et al.* (1995) Failure of postsynaptic specialisation to develop at neuromuscular junctions of rapsyn-deficient mice. *Nature* 377, 232–236
37 Grady, R.M. *et al.* (2000) Maturation and maintenance of the neuromuscular synapse: Genetic evidence for roles of the dystrophin-glycoprotein complex. *Neuron* 25, 279–293
38 Sotgia, F. *et al.* (2000) Caveolin-3 directly interacts with the c-terminal tail of β-dystroglycan: identification of a central WW-like domain within caveolin family members. *J. Biol. Chem.* 275, 38048–38058
39 Galbiati, F. *et al.* (2000) Transgenic overexpression of caveolin-3 in skeletal muscle fibers induces a Duchenne-like muscular dystrophy phenotype. *Proc. Natl. Acad. Sci. U. S. A.* 97, 9689–9694
40 Bredt, D.S. (1999) Knocking signalling out of the dystrophin complex. *Nat. Cell Biol.* 1, E89–E91
41 Gee, S.H. *et al.* (1998) Interaction of muscle and brain sodium channels with multiple members of the syntrophin family of dystrophin-associated proteins. *J. Neurosci.* 18, 128–137
42 Yoshida, T. *et al.* (1998) Bidirectional signaling between sarcoglycans and the integrin adhesion system in cultured L6 myoblasts. *J. Biol. Chem.* 273, 1583–1590
43 Cavaldesi, M. *et al.* (1999) Association of the dystroglycan complex isolated from bovine brain synaptosomes with proteins involved in signal transduction. *J. Neurochem.* 72, 1648–1655
44 Yang, B. *et al.* (1995) SH3 domain-mediated interaction of dystroglycan and Grb2. *J. Biol. Chem.* 270, 11711–11714
45 Belkin, A.M. and Burridge, K. (1995) Localization of utrophin and aciculin at sites of cell-matrix and cell-cell adhesion in cultured cells. *Exp. Cell Res.* 221, 132–140
46 Belkin, A.M. and Smallheiser, N.R. (1996) Localization of cranin (dystroglycan) at sites of call-matrix and cell-cell contact: recruitment to focal adhesions is dependent upon extracellular ligands. *Cell Adhes. Commun.* 4, 281–296
47 James, M. *et al.* (1996) Utrophin-dystroglycan complex in membranes of adherent cultured cells. *Cell Motil. Cytoskel.* 33, 163–174
48 Hemler, M.E. *et al.* (1996) Association of TM4SF proteins with integrins: Relevance to cancer. *Biochim. Biophys. Acta* 1287, 67–71
49 Crosbie, R.H. *et al.* (1997) Sarcospan, the 25 kDa transmembrane component of the dystrophin–glycoprotein complex. *J. Biol. Chem.* 272, 31221–31224
50 Culligan, K.G. *et al.* (1998) Role of dystrophin isoforms and associated proteins in muscular dystrophy. *Int. J. Mol. Med.* 2, 639–648
51 Salih, M.A. *et al.* (1996) Muscular dystrophy associated with β-dystroglycan deficiency. *Ann. Neurol.* 40, 925–928
52 Rambukkana, A. *et al.* (1998) Role of α-dystroglycan as a Schwann cell receptor for *Mycobacterium leprae*. *Science* 282, 2076–2079
53 Cao, W. *et al.* (1998) Identification of α-dystroglycan as a receptor for lymphocytic choriomeningitis virus and Lassa fever virus. *Science* 282, 2079–2081
54 Lim, L.E. and Campbell, K.P. (1998) The sarcoglycan complex in limb-girdle muscular dystrophy. *Curr. Opin. Neurol.* 11, 443–452
55 Kachinsky, A.M. *et al.* (1999) A PDZ-containing scaffold related to the dystrophin complex at the basolateral membrane of epithelial cells. *J. Cell Biol.* 145, 391–402
56 Tinsley, J.M. *et al.* (1996) Amelioration of the dystrophic phenotype of *mdx* mice using a truncated utrophin transgene. *Nature* 384, 349–353
57 Lowenstein, E.J. *et al.* (1992) The SH2 and SH3 domain containing protein GRB2 links receptor tyrosine kinases to ras signaling. *Cell* 70, 431–442
58 Hoch, W. (1999) Formation of the neuromuscular junction – Agrin and its unusual receptors. *Eur. J. Biochem* 265, 1–10
59 Colognato, H. and Yurchenco, P.D. (2000) Form and function: the laminin family of heterotrimers. *Dev. Dyn.* 218, 213–234
60 Iozzo, R.V. (1998) Matrix proteoglycans: from molecular design to cellular function. *Annu. Rev. Biochem.* 67, 609–652
61 Holt, K.H. *et al.* (2000) Biosynthesis of dystroglycan: processing of a precursor propeptide. *FEBS Lett.* 468, 79–83
62 Brancaccio, A. *et al.* (1995) Electron microscopic evidence for a mucin-like region in chick muscle α-dystroglycan. *FEBS Lett.* 368, 139–142

Ribosome fidelity: tRNA discrimination, proofreading and induced fit

Marina V. Rodnina and Wolfgang Wintermeyer

The ribosome selects aminoacyl-tRNAs with high fidelity. Kinetic studies reveal that codon–anticodon recognition both stabilizes aminoacyl-tRNA binding on the ribosome and accelerates reactions of the productive pathway, indicating an important contribution of induced fit to substrate selection. Similar mechanisms are used by other template-programmed enzymes, such as DNA and RNA polymerases.

High fidelity substrate selection is crucial in the transmission and expression of genetic information. The nucleic acid-programmed enzymes involved in these processes, such as DNA/RNA polymerases and ribosomes, discriminate effectively between structurally similar substrates, nucleoside triphosphates (NTPs) and aminoacyl-tRNAs (aa-tRNAs), respectively, on the basis of complementary base pairing with the respective templates. During mRNA translation into protein, the ribosome selects the correct aminoacyl-tRNA (aa-tRNA), in the form of a ternary complex with elongation factor Tu (EF-Tu) and GTP, from the many incorrect ones, on the basis of the match between codon and anticodon triplets. In the cognate complex, three base pairs are formed between codon and anticodon, whereas in near- and non-cognate cases the match is imperfect, ranging from a single mismatch to no base pair at all. The

http://tibs.trends.com 0968-0004/01/$ – see front matter PII: S0968-0004(00)01737-0

free energy difference $\Delta\Delta G^{\circ}$ between cognate and near-cognate base pairs can be small, about 3 kcal mol^{-1} or less, predicting an error frequency of up to one out of 100 amino acids incorporated. However, significantly lower error frequencies are found *in vivo*, ranging from 6×10^{-4} to 5×10^{-3} on internal mRNA codons in *Escherichia coli* (Ref. 1). To resolve the discrepancy, kinetic proofreading models were proposed in which the same discriminatory interaction is used more than once in consecutive selection steps that are separated by irreversible energy-dissipating reactions[2,3].

This review summarizes the present knowledge on kinetic proofreading mechanisms during aa-tRNA selection on the ribosome. The emphasis is on the importance of induced fit and on structural elements of the ribosome that might be affected. A brief discussion of induced-fit mechanisms used by DNA and RNA polymerases is included for comparison. Editing mechanisms by which incorrectly formed products are discarded hydrolytically, for instance, by DNA polymerases or aa-tRNA synthetases, are not included. For information regarding aa-tRNA synthetases, including the structural characterization of the domain comprising the hydrolytic active site, see Refs 4–6.

For translation on the ribosome, the kinetic proofreading model was verified by Thompson and colleagues[7], and later confirmed by Ehrenberg, Kurland and colleagues[8]. Their kinetic experiments have established that the selection of aa-tRNAs by the ribosome is accomplished in two steps: initial selection and proofreading, which are separated by GTP hydrolysis. In their pioneering work, Thompson and colleagues introduced single-turnover kinetics to measure rates of GTP hydrolysis and peptide bond formation[9], demonstrating that discrimination in both selection steps is based on different stabilities of correct and incorrect codon–anticodon duplexes[10]. However, these data alone were not sufficient to explain quantitatively the experimentally observed error .

Recently, the complete kinetic mechanism of aa-tRNA binding was established[11] (Fig. 1). First, the ternary complex of aa-tRNA with EF-Tu–GTP binds to the ribosome and forms a readily reversible initial binding complex that dissociates rapidly when there is no match between anticodon and codon. When a codon is recognized, the complex is stabilized and EF-Tu undergoes a conformational rearrangement towards the active state for GTP hydrolysis (GTPase activation). After GTP hydrolysis, EF-Tu rearranges from the GTP- to the GDP-bound form, thereby loosing the affinity for aa-tRNA. The aminoacyl end of aa-tRNA is then free to move into the peptidyl transferase center on

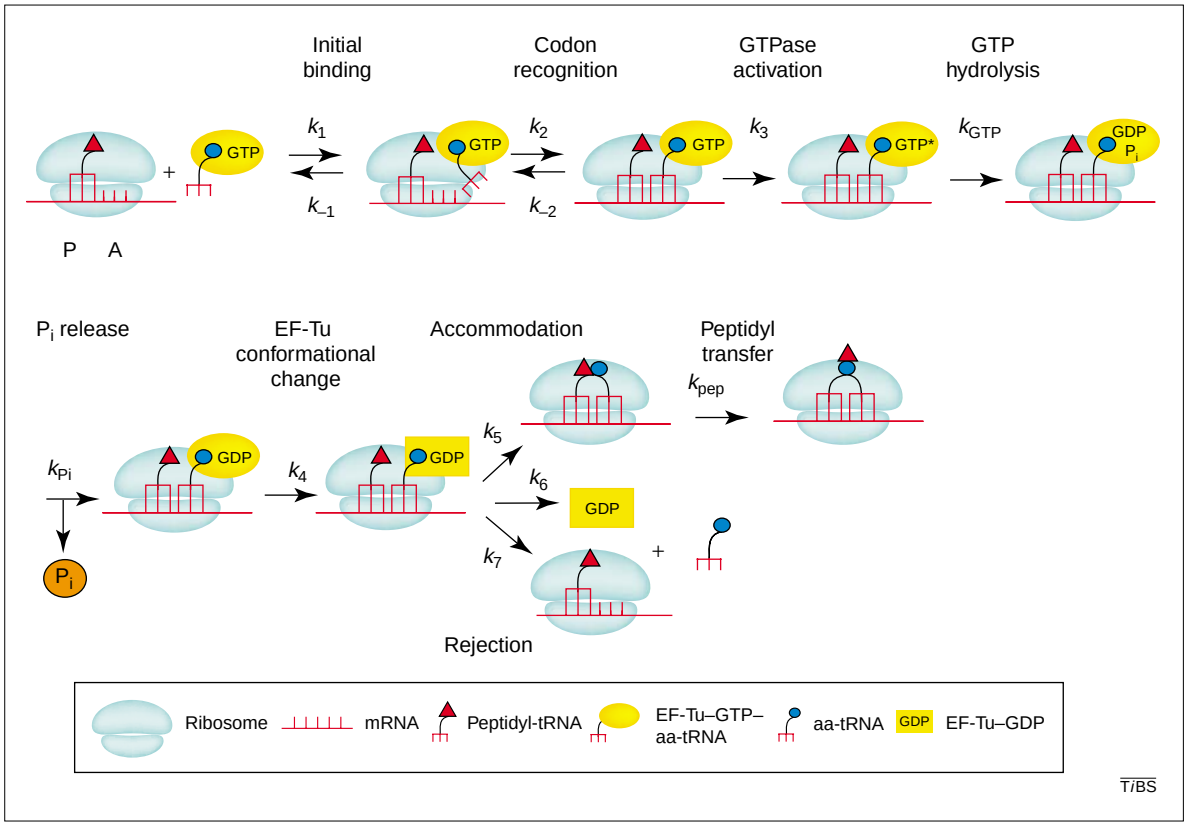

Fig. 1. Kinetic mechanism of aa-tRNA binding to the A site of the ribosome. Kinetically resolved steps are indicated by numbered rate constants, steps that are rate-limited by the preceding step are designated k_{GTP}, k_{Pi}, and k_{pep}. The binding sites of the ribosome for peptidyl-tRNA and aminoacyl-tRNA (aa-tRNA) are designated P and A, respectively. Elongation factor Tu (EF-Tu) is depicted differently in the GTP- and GDP-bound conformations, GTP* denotes the GTPase state. Abbreviation: P_i, inorganic phosphate.

Marina V. Rodnina*
Wolfgang Wintermeyer
Institutes of Physical Biochemistry and Molecular Biology, University of Witten/Herdecke, 58448 Witten, Germany.
*e-mail: rodnina@uni-wh.de

the 50S subunit (accommodation), where it takes part in peptide bond formation. Alternatively, aa-tRNA can dissociate from the ribosome. In addition, kinetic mechanisms were solved for near-cognate and non-cognate aa-tRNAs (Refs 12,13), allowing for the quantitative description of the mechanisms operating in aa-tRNA selection.

Two selection steps in aa-tRNA discrimination

The selection of aa-tRNA in response to the codon in the ribosomal A site takes place before GTP hydrolysis (initial selection) and after GTP hydrolysis but before peptide bond formation (proofreading). Non-cognate ternary complexes are efficiently excluded in the initial selection step (Fig. 2). The efficiency of initial selection is determined by the rate constants of initial binding k_1 and k_{-1}, of codon recognition k_2 and k_{-2}, and of GTP hydrolysis k_{GTP}. The association rate constants k_1 were found to be similar for cognate, near-cognate and non-cognate ternary complexes[12]. Therefore, all ternary complexes have the same chance to bind to the ribosome initially, irrespective of the codon present in the A site. In the initial binding complex, the anticodon is screened for codon recognition and, when there is a significant match between anticodon and codon, the ternary complex is stabilized on the ribosome (slow k_{-2}). In non-cognate cases, when base pairing is insufficient, the ternary complex dissociates from the ribosome before GTP hydrolysis (slow k_3). Thus, the bulk of non-cognate ternary complexes is discriminated in a single selection step with essentially no cost with respect to GTP hydrolysis[13].

Discrimination against near-cognate ternary complexes requires a more complex mechanism (Fig. 3). Upon codon recognition, near-cognate aa-tRNA is stabilized (k_{-2}) and the hydrolysis of GTP in EF-Tu is stimulated (k_3), although not to the same extent as in the cognate case. Although k_{-2} differs approximately 100-fold between cognate and near-cognate ternary complexes, initial selection is not very effective because this difference is outweighed by the increase of k_3, such that rapid and irreversible GTP hydrolysis largely precludes the equilibration of the preceding reversible steps. The efficiency of initial selection is influenced by the Mg^{2+} concentration and ranges from low (10 mM Mg^{2+}; Fig. 3) to about 1:10 at conditions closer to physiological ones (5 mM Mg^{2+})[13]. The majority of near-cognate aa-tRNA rejection takes place in the subsequent proofreading step. Because the near-cognate codon–anticodon complex is less stable than the cognate one, there is a higher probability that near-cognate aa-tRNA will dissociate from the ribosome at this stage (k_7; Fig. 3). In previous models, discrimination by rejection during both initial selection and proofreading was attributed exclusively to those differences in dissociation rates[10]. It is important to note, however, that the probability of being rejected during the proofreading phase is increased for the near-cognate aa-tRNA because the accommodation step (k_5) is much slower with the near-cognate than with the cognate aa-tRNA. A similar effect is noted for the GTPase activation step (k_3) in the initial selection phase. The efficiency of rejection in the proofreading step is determined by the ratio of the rate constants of rejection and accommodation k_7:k_5. This ratio is 60 for the near-cognate and <0.04 for the cognate aa-tRNA (Fig. 3), meaning that there is efficient rejection of the former and practically no rejection of the latter. These values are probably representative of the *in vivo* situation, because the proofreading step is not much influenced by the buffer conditions[13].

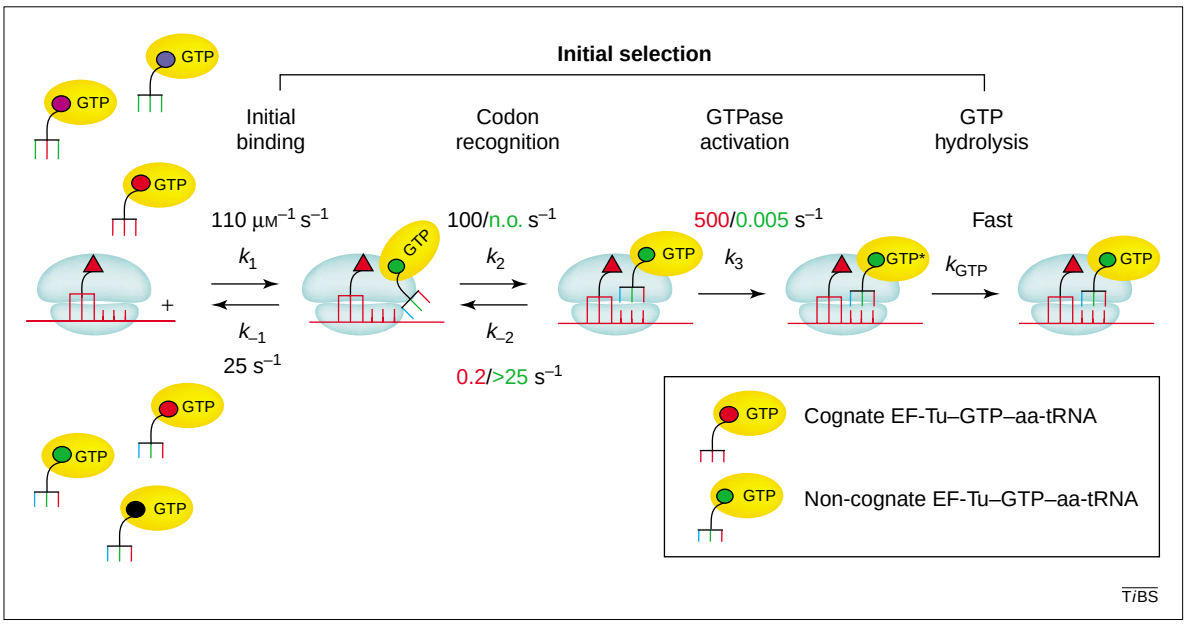

Fig. 2. Discrimination against non-cognate ternary complexes. Black, rate constants that are the same for cognate and non-cognate aa-tRNA and hence do not contribute to discrimination; red, rate constants that are specific for cognate aa-tRNA; green, rate constants for non-cognate aa-tRNA. The rate constants for cognate aa-tRNA, Phe-$tRNA^{Phe}$ (anticodon 3′-AAG-5′) on a UUU codon are taken from Ref. 11; those for non-cognate Phe-$tRNA^{Phe}$(AAG) and Leu-$tRNA^{Leu2}$(GAG) on an AAA codon are from Ref. 12. Rate constants are for 10 mM Mg^{2+} and 20 °C. GTP* denotes the GTPase state. Abbreviation: n.o., not observed.

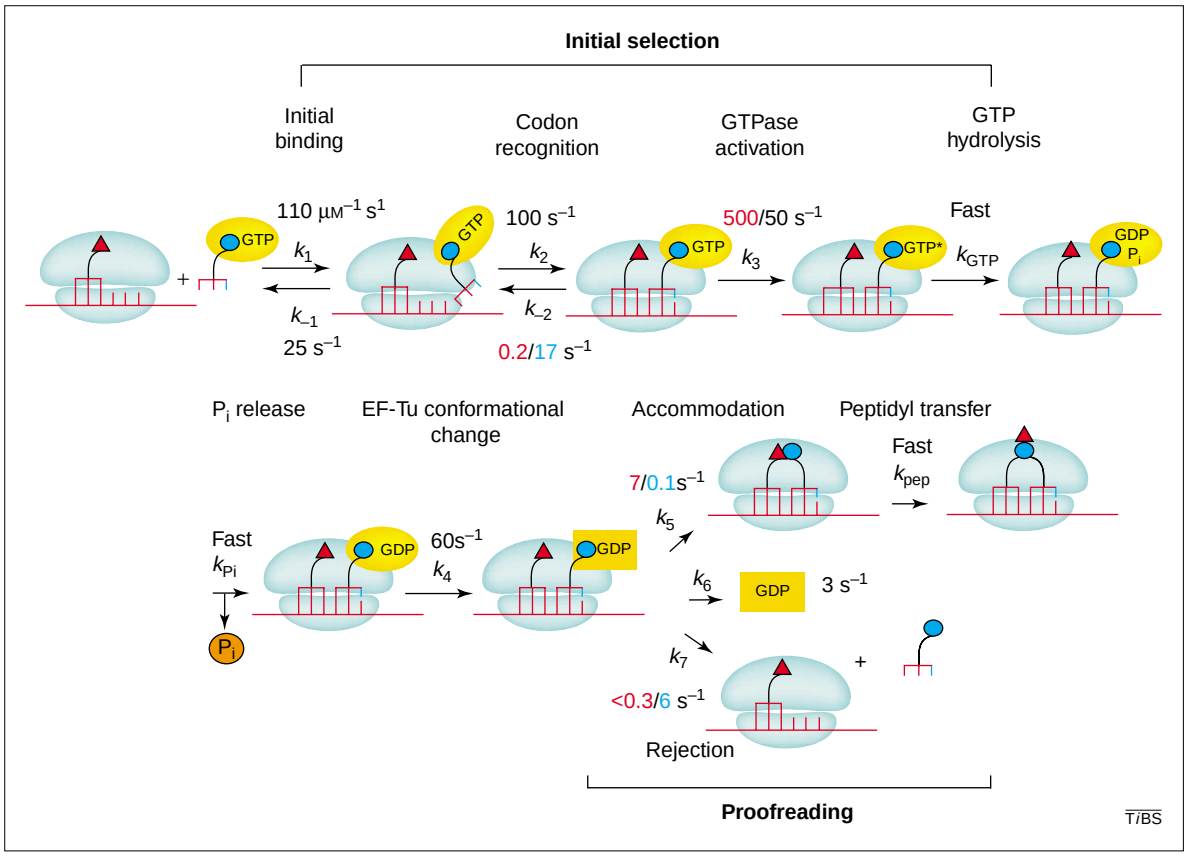

Fig. 3. Discrimination against near-cognate ternary complexes. Black, rate constants that are the same for cognate and near-cognate aa-tRNA; red, rate constants that are specific for cognate aa-tRNA; blue, rate constants for near-cognate aa-tRNA. The rate constants for cognate Phe-tRNA^{Phe}(AAG) and near-cognate Leu-tRNA^{Leu2} (GAG) on a UUU codon were determined at 10 mM Mg^{2+} and 20 °C (Ref. 13). GTP* denotes the GTPase state. Abbreviation: P_i, inorganic phosphate.

Strategies for substrate selection: discrimination by stability and induced fit

Discriminating between two substrates based on their affinity to the enzyme appears to be an obvious strategy to use. Indeed, the different stabilities of correct and incorrect codon–anticodon pairs are used in both phases of selection on the ribosome. However, the ribosome uses yet another discrimination strategy. The correct codon–anticodon interaction not only slows the dissociation rate, but also greatly accelerates two forward reactions, GTPase activation and accommodation, and the subsequent irreversible chemistry steps. Thus, the ribosome uses an induced-fit mechanism for improving the selection of the correct aa-tRNA and the discrimination against the incorrect ones. The ribosome seems to assume two different conformations: a binding conformation that accepts or rejects substrates on the basis of different binding stabilities, and a productive conformation that favors GTP hydrolysis and peptide bond formation. The productive conformation is induced by correct base pairing between codon and anticodon, and is inhibited by mismatches in the codon–anticodon complex.

According to the theory of induced fit: (1) the precise orientation of the catalytic groups is required for enzyme action; (2) the binding of the correct substrate causes a change in the 3D structure of the active site towards the active state; and (3) binding of an incorrect substrate to the active site does not induce these changes[14]. Substrate-induced conformational changes have been found for many enzymes. However, the question remains whether induced fit improves specificity. A simple Michaelis–Menten enzyme binds its substrates rapidly, whereas k_{cat} is determined by a subsequent slow step. With such an enzyme, substrate-induced conformational changes would affect equally the relative catalytic efficiency towards the two substrates and thus would not improve specificity[15]. This conclusion is valid for cases where there is a single active conformation of the enzyme, such as when the alignment of the catalytic groups is required to be identical for any substrate to react. However, the kinetic data show that this is not the case for aa-tRNA binding to the A site, because the rates of the two chemical steps, GTP hydrolysis and peptide bond formation, are lower for the incorrect substrates than for the correct ones.

The more general formulation of the reaction pathway for an induced-fit enzyme allows different substrates to induce non-identical forms of the activated enzyme such that substrate-dependent conformational differences prevail in the transition state. In such cases, the catalytic efficiency towards two substrates can be different, originating in part from specific, substrate-induced conformational changes and thereby enhancing substrate specificity[16]. There are other special cases where conformational changes do improve specificity, for example when the binding step is rate limiting for the correct substrate and the chemical step is rate limiting for an incorrect substrate[17,18]. The kinetic analysis reveals that the

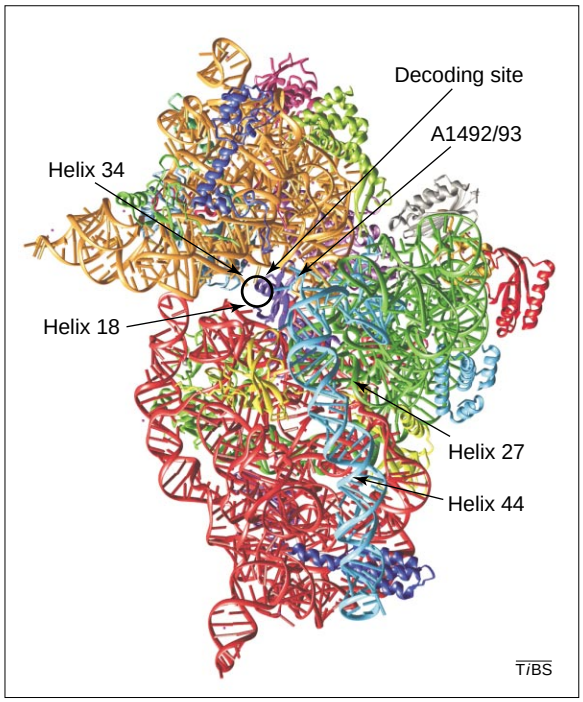

Fig. 4. Crystal structure of the 30S ribosomal subunit from *Thermus thermophilus*. The locations of the decoding site and of structural elements mentioned in the text are indicated. Different domains of 16S rRNA are color-coded as follows: red, 5′-domain; green, central domain; orange, 3′-major domain; cyan, 3′-minor domain. Ribosomal proteins are shown in various colors. The figure was kindly provided by V. Ramakrishnan (MRC Laboratory of Molecular Biology, Cambridge, UK).

ribosome uses both strategies for substrate discrimination, in that it selects its substrates on the basis of both different binding energies and different effects on catalysis of correct and incorrect substrates.

Ribosome structure and fidelity

The induced-fit model implies that the formation of the correct codon–anticodon complex induces a structural change of the decoding center on the 30S ribosomal subunit. This change in structure is communicated to the 50S subunit, where both the GTPase activating center and the peptidyl transferase center are located. It is not known how the ribosome senses structural differences between correct and incorrect codon–anticodon duplexes on the 30S subunit, nor is it known how these differences affect the GTPase activation and accommodation steps on the 50S subunit. In examining the codon–anticodon complex, the ribosome has to distinguish correctly paired bases from mismatches in a sequence-independent manner. It is possible that the ribosome senses the geometry of the sugar-phosphate backbone of the codon–anticodon helix that is affected by mismatches. Another possibility is provided by the fact that in all Watson–Crick base pairs, N3 of purine bases and O2 of pyrimidine bases assume the same position, thus providing the same sequence-independent pattern of potential hydrogen bond acceptors[19]. By donating hydrogen bonds to those acceptors, ribosomal residues of the decoding center might establish interactions preferentially with correct base pairs, thereby sensing the correct codon–anticodon complex on the ribosome.

One candidate to form direct interactions with the codon–anticodon complex is helix 44 of 16S rRNA (nucleotides 1400–1500), as deduced from footprinting[20,21] and mutational analyses[22]. According to the high-resolution (3.0–3.3 Å) crystal structures of the 30S subunit (Fig. 4)[23,24], the decoding site is mainly composed of RNA, including helices 18 and 34 as well as adenines 1492 and 1493 of helix 44. The only protein that is located close to the site of codon–anticodon interaction is S12. According to a model derived from the crystal structure[25], adenines 1492 and 1493 can interact with the minor groove of the codon–anticodon double helix and form hydrogen bonds with 2′-OH groups of the backbone on both sides of the duplex. The hydrogen bonds can be formed with positions N1, N6 and N3, or N1, N6 and N7 of adenines 1492 and 1493. The latter mode of interaction, which is supported by mutational analysis[26], would allow the formation of sequence-independent hydrogen bonds of adenine N6 with O2 and N3 in the codon–anticodon helix. Additional interactions with the codon–anticodon helix might be provided by helices 18 and 34, both of which are known to influence accuracy[22,27,28].

In the 7.8 Å crystal structure of the 70S ribosome carrying a tRNA in the A site, the part of helix 44 that forms the A site of the decoding center, including nucleotides 1492 and 1493, is about 15 Å apart from the site of codon–anticodon interaction, which seems too far for the interactions in question[29]. Although it is possible that the latter structure represents a different state of the ribosome compared with the structure of isolated 30S subunits, higher resolution is required to see structural details around the codon–anticodon double helix in the decoding center.

It appears likely that the structure of the decoding center changes when interactions between ribosomal residues and the codon–anticodon duplex are formed, thus creating a conformational signal that could be communicated to distant parts of the ribosome where GTP hydrolysis and peptidyl transfer are controlled. In fact, the conformational dynamics of the decoding region (helix 44) seem to play an important role in modulating fidelity. A model RNA comprising the decoding center can assume two different conformations in solution, one of which is stabilized by the antibiotic paromomycin, which is known to enhance misreading[30]. Interestingly, this paromomycin-induced conformation of the 16S decoding region was observed in the crystal structure of ribosome complexes with tRNA bound to the A site[29].

A kinetic analysis has revealed that paromomycin stabilizes the binding of aa-tRNA in the A site, irrespective of whether the codon–anticodon pair is cognate or near-cognate, and accelerates both GTP hydrolysis and peptide bond formation[31], hence the increased amino acid misincorporation. Furthermore, the antibiotic decreases the rate of

codon recognition, suggesting that binding of the antibiotic induces a rearrangement from a binding to a productive conformation of the decoding region. The conclusion is that cognate codon–anticodon recognition, or near-cognate codon recognition augmented by antibiotic binding, promotes the rearrangement of 16S rRNA towards the productive conformation.

Another region of 16S rRNA that is involved in fidelity control is helix 27. This helix was shown to exist in two alternative base-paired arrangements which, when stabilized by mutations, either increase or decrease accuracy[32]. Ribosomal proteins might be involved as well. Mutations in protein S12 confer resistance to or dependence on the error-inducing antibiotic streptomycin, retard translation rate and increase accuracy. Mutations in ribosomal proteins S4 and S5 confer the opposite phenotype, because they increase the basal translational error rate and can suppress the streptomycin dependence of restrictive S12 mutants. Ribosomal proteins S4, S5 and S12 protect nucleotides in helix 27 from chemical modification, and mutations in the three proteins alter the structure of the region and modulate the conformation of helix 27 (Ref. 32). Helix 27 might be involved in transmitting the signal from the decoding site to the functional sites on the 50S subunit. In the crystal structures of the 70S ribosome[29] and the isolated 30S ribosomal subunit[23,24], helix 27 is about 15 Å away from the anticodon of the A site-bound tRNA, making a direct interaction with the codon–anticodon complex in the A site unlikely. However, the switch in helix 27 might induce cooperative opening and closing of RNA helices in the vicinity of the decoding center[29,32], such as helices 44, 18 and 34, thereby altering the positions and/or interactions of proteins S4, S5 and S12. In fact, major rearrangements in the structure of 70S ribosomes were observed in reconstructions obtained by cryo-electron microscopy (cryo-EM), when a particular conformation of 16S rRNA was stabilized by mutations in helix 27 (Ref. 33). Alternatively, because the penultimate stem of helix 27 and the closing 900 loop are involved in the communication between 30S and 50S subunits[29,34], the switch between two conformations in this region might be instrumental in transmitting the conformational signal to the 50S subunit.

For 23S rRNA in the large ribosomal subunit, several fidelity mutations have been described. These mutations are located in helix 69 in domain IV, in helix 89 in domain V, and in the sarcin-ricin loop (SRL) in domain VI of 23S rRNA (Refs 35,36). These regions of 23S rRNA are involved in different functions. Helix 69 forms an intersubunit bridge to the decoding part of helix 44 in 16S rRNA[29], suggesting that mutations in helix 69 interfere with the communication between subunits. Helix 89 is located in the vicinity of the peptidyl transferase center of the ribosome[37,38], and it is conceivable that mutations in this region, by changing its structure, affect the accuracy of amino acid incorporation by influencing the accommodation of aa-tRNA or peptide bond formation, or both. Finally, mutations in the SRL are likely to influence the interaction of the ribosome with EF-Tu (Ref. 39), thereby affecting partial reactions of A-site binding in an as yet unknown way.

In conclusion, three groups of structural elements of the ribosome influence the fidelity of protein synthesis. The first group includes those regions of 16S rRNA and proteins of the small ribosomal subunit that form the decoding region. These elements are likely to be involved directly or indirectly in sensing the structure of the codon–anticodon complex and in creating the conformational signal of codon recognition. The second group includes parts of rRNA at the subunit interface that might mediate the transmission of the conformational signal from the 30S decoding site to the active center(s) on the 50S subunit. Finally, the third group comprises regions of the 50S subunit that might receive and convert the signal by accelerating GTPase activation and aa-tRNA accommodation. Mutations in those elements of the ribosome appear to change the relative rates of productive versus rejection reactions during aa-tRNA selection and, thereby, influence accuracy.

Induced fit in other template-programmed polymerases

Most enzymes possess active sites that are tailored specifically to the structure of the correct substrate or its transition state and will not accept incorrect substrates. However, this is not an adequate discrimination strategy for enzymes that synthesize polymers from structurally similar monomeric substrates. Like ribosomes, DNA and RNA polymerases recognize their NTP substrates on the basis of complementary base pairing to a nucleic acid template. This means that the structure of the correct substrate, as defined by the template, can differ from cycle to cycle. DNA polymerases catalyse the incorporation of nucleotides with low error frequency (10^{-5}–10^{-6}). In addition, when an incorrect nucleotide has been incorporated, the polymerase activity of the enzyme is slowed down, which gives the time to correct the error by exonucleolytically removing the mismatched nucleotide, such that the overall error frequency approaches 10^{-8}–10^{-10} (Ref. 18). The low error of nucleotide incorporation is, in part, achieved by induced fit. NTP binding to DNA polymerase is a two-step process: initially an ‘open’, relatively weak complex is formed in which the rate of incorporation is low. Binding of the correct NTP, but not of the incorrect one, triggers the transition into a ‘closed’ state that both tightens the binding and accelerates

the incorporation[18,40]. The crystal structures of DNA polymerase complexes with template-primer DNA and NTP substrate analogs suggest that residues of the enzyme contribute to the fidelity of DNA synthesis by recognizing correct base pairs[41,42], and indicate how the transition between the open and closed forms of DNA polymerase take place[19,43]. A similar mechanism appears to operate in *E. coli* RNA polymerase[44,45]. This is a type of induced-fit mechanism in which binding of the incorrect substrate impedes the conformational change that converts the polymerase from the inactive (open) to the active (closed) form. Similar mechanisms appear to be used by the ribosome, indicating that the same kinetic mechanisms have evolved to attain the high fidelity of template-dependent polymerases.

Concluding remarks

The kinetic analysis of the mechanism of aa-tRNA selection on the ribosome has revealed that the discrimination of correct and incorrect substrates is achieved in two consecutive steps, initial selection and proofreading, which operate on the basis of both substrate stabilities and induced fit. The mechanism of ribosomal selection is similar to the mechanisms used by other template-dependent enzymes, such as DNA and RNA polymerases. The structural determinants that sense the cognate base pairing on the ribosome, and the relay mechanisms of intersubunit communication are not yet clear. Future challenges are to identify the residues of the ribosome that contribute to recognition and to study the kinetics of the interplay between the different discrimination strategies for the regulation of translational fidelity.

Acknowledgements
The authors thank V. Ramakrishnan for kindly providing the 30S structure and J. Pleiss for valuable comments on the manuscript. This work was supported by the Deutsche Forschungsgemeinschaft and the Alfried Krupp von Bohlen und Halbach-Stiftung.

References

1 Kurland, C.G. and Ehrenberg, M. (1987) Growth-optimizing accuracy of gene expression. *Annu. Rev. Biophys. Biophys. Chem.* 16, 291–318
2 Hopfield, J.J. (1974) Kinetic proofreading: A new mechanism for reducing errors in biosynthetic processes requiring high specificity. *Proc. Natl. Acad. Sci. U. S. A.* 71, 4135–4139
3 Ninio, J. (1975) Kinetic amplification of enzyme discrimination. *Biochimie* 57, 587–595
4 Nomaboy, T.K. *et al.* (1999) Transfer RNA-dependent translocation of misactivated amino acids to prevent errors in protein synthesis. *Mol. Cell* 4, 519–528
5 Silvian, L.F. *et al.* (1999) Insights into editing from an Ile-tRNA synthetase structure with $tRNA^{Ile}$ and mupirocin. *Science* 285, 1074–1077
6 Sankaranarayanan, R. *et al.* (2000) Zink ion mediated amino acid discrimination by threonyl-tRNA synthetases. *Nat. Struct. Biol.* 7, 461–465
7 Thompson, R.C. and Stone, P.J. (1977) Proofreading of the codon–anticodon interaction on ribosomes. *Proc. Natl. Acad. Sci. U. S. A.* 74, 198–202
8 Ruusala, T. *et al.* (1982) Is there proofreading during polypeptide synthesis? *EMBO J.* 1, 741–745
9 Eccleston, J.F. *et al.* (1985) The rate of cleavage of GTP on the binding of Phe-tRNA·elongation factor Tu·GTP to poly(U)-programmed ribosomes of *Escherichia coli*. *J. Biol. Chem.* 260, 16237–16241
10 Thompson, R.C. (1988) EF-Tu provides an internal kinetic standard for translational accuracy. *Trends Biochem. Sci.* 13, 91–93
11 Pape, T. *et al.* (1998) Complete kinetic mechanism of elongation factor Tu-dependent binding of aminoacyl-tRNA to the A site of the *E. coli* ribosome. *EMBO J.* 17, 7490–7497
12 Rodnina, M.V. *et al.* (1996) Initial binding of the elongation factor Tu·GTP·aminoacyl-tRNA complex preceding codon recognition on the ribosome. *J. Biol. Chem.* 271, 646–652
13 Pape, T. *et al.* (1999) Induced fit in initial selection and proofreading of aminoacyl-tRNA on the ribosome. *EMBO J.* 18, 3800–3807
14 Koshland, D.E. (1958) Application of a theory of enzyme specificity to protein synthesis. *Proc. Natl. Acad. Sci. U. S. A.* 44, 98–104
15 Fersht, A. (1998) *Structure and Mechanism in Protein Science*, W.H. Freeman
16 Post, C.B. and Ray, W.J. (1995) Reexamination of induced fit as determinant of substrate specificity in enzymatic reactions. *Biochemistry* 34, 15881–15890
17 Herschlag, D. (1988) The role of induced fit and conformational changes of enzymes in specificity and catalysis. *Bioorg. Chem.* 16, 62–96
18 Johnson, K.A. (1993) Conformational coupling in DNA polymerase fidelity. *Annu. Rev. Biochem.* 62, 685–713
19 Doublié, S. and Ellenberger, T. (1998) The mechanism of action of T7 DNA polymerase. *Curr. Opin. Struct. Biol.* 8, 704–712
20 Purohit, P. and Stern, S. (1994) Interactions of a small RNA with antibiotic and RNA ligands of the 30S subunit. *Nature* 370, 659–662
21 Moazed, D. and Noller, H.F. (1990) Binding of tRNA to the ribosomal A and P sites protects two distinct sets of nucleotides in 16 S rRNA. *J. Mol. Biol.* 211, 135–145
22 O'Connor, M. *et al.* (1997) Decoding fidelity at the ribosomal A and P sites: influence of mutations in three different regions of the decoding domain in 16S rRNA. *Nucleic Acids Res.* 25, 1185–1193
23 Wimberly, B.T. *et al.* (2000) Structure of the 30S ribosomal subunit. *Nature* 407, 327–339
24 Schluenzen, F. *et al.* (2000) Structure of functionally activated small ribosomal subunit at 3.3 Å resolution. *Cell* 102, 615–623
25 Carter, A.P. *et al.* (2000) Functional insights from the structure of the 30S ribosomal subunit and its interactions with antibiotics. *Nature* 407, 340–348
26 Yoshizawa, S. *et al.* (1999) Recognition of the codon–anticodon helix by ribosomal RNA. *Science* 285, 1722–1725
27 Van Ryk, D.I. and Dahlberg, A.E. (1995) Structural changes in the 530 loop of *Escherichia coli* 16S rRNA in mutants with impaired translational fidelity. *Nucleic Acids Res.* 23, 3563–3570
28 Powers, T. and Noller, H.F. (1994) The 530 loop of 16S rRNA: a signal to EF-Tu? *Trends Genet.* 10, 27–31
29 Cate, J.H. *et al.* (1999) X-ray crystal structures of 70S ribosome functional complexes. *Science* 285, 2095–2104
30 Fourmy, D. *et al.* (1998) Paromomycin binding induces a local conformational change in the A-site of 16 S rRNA. *J. Mol. Biol.* 277, 333–345
31 Pape, T. *et al.* (2000) Conformational switch in the decoding region of 16S rRNA during aminoacyl-tRNA selection on the ribosome. *Nat. Struct. Biol.* 7, 104–107
32 Lodmell, J.S. and Dahlberg, A.E. (1997) A conformational switch in *Escherichia coli* 16S ribosomal RNA during decoding of messenger RNA. *Science* 277, 1262–1267
33 Gabashvili, I.S. *et al.* (1999) Major rearrangements in the 70S ribosomal 3D structure caused by a conformational switch in 16S ribosomal RNA. *EMBO J.* 18, 6501–6507
34 Gabashvili, I.S. *et al.* (2000) Solution structure of the *E. coli* 70S ribosome at 11.5 Å resolution. *Cell* 100, 537–549
35 O'Connor, M. and Dahlberg, A.E. (1995) The involvement of two distinct regions of 23S ribosomal RNA in tRNA selection. *J. Mol. Biol.* 254, 838–847
36 Gregory, S.T. *et al.* (1994) Mutations in the peptidyl transferase region of *E. coli* 23S rRNA affecting translational accuracy. *Nucl. Acids Res.* 22, 279–284
37 Ban, N. *et al.* (2000) The complete atomic structure of the large ribosomal subunit at 2.4 Å resolution. *Science* 289, 905–920
38 Nissen, P. *et al.* (2000) The structural basis of ribosome activity in peptide bond synthesis. *Science* 289, 920–930
39 Tapprich, W.E. and Dahlberg, A.E. (1990) A single base mutation at position 2661 in *E. coli* 23S ribosomal RNA affects the binding of ternary complex to the ribosome. *EMBO J.* 9, 2649–2655
40 Rittinger, K. *et al.* (1995) Human immunodeficiency virus reverse transcriptase substrate-induced conformational changes and the mechanism of inhibition by nonnucleoside inhibitors. *Proc. Natl. Acad. Sci. U.S.A.* 92, 8046–8049
41 Doublié, S. *et al.* (1998) Crystal structure of bacteriophage T7 DNA replication complex at 2.2 Å. *Nature* 391, 251–259
42 Kiefer, J.R. *et al.* (1998) Visualizing DNA replication in a catalytically active Bacillus DNA polymerase crystal. *Nature* 391, 304–307
43 Li, Y. *et al.* (1998) Crystal structures of open and closed forms of binary and ternary complexes of the large fragment of *Thermus aquaticus* DNA polymerase I: structural basis for nucleotide incorporation. *EMBO J.* 17, 7514–7525
44 Erie, D.A. *et al.* (1993) Multiple RNA polymerase conformations and GreA: control of the fidelity of transcription. *Science* 262, 867–873
45 Thomas, M.J. *et al.* (1998) Transcriptional fidelity and proofreading by RNA polymerase II. *Cell* 93, 627–637